A molecular dynamics study of void interaction in copper

2010 IOP Conf. Ser.: Mater. Sci. Eng. 10 012175

(http://iopscience.iop.org/1757-899X/10/1/012175)

IOP Conf. Series: Materials Science and Engineering **10** (2010) 012175 doi:10.1088/1757-899X/10/1/012175

A molecular dynamics study of void interaction in copper

S Z Xu*, Z M Hao and Q Wan

Institute of Structural Mechanics, China Academy of Engineering Physics, Mian Yang, P R China

E-mail: * shuozhixu@gmail.com

Abstract. Molecular dynamics simulations in three-dimensional single crystal copper under remote uniaxial tension at high strain rate (10^9/s) were performed to analyze the microscopic mechanism of dislocation emission and void interaction. Two different cases, characterized by whether the line joining centers of two embedded cylindrical voids was perpendicular to or paralleled the tension direction, were studied using embedded atom method (EAM) potentials. The mean-squared displacements of atoms around the voids marking both yielding and coalescence points were presented. The critical position of the first slide was predicted where shear stress at slip plane was maximum.

1. Introduction

Ductile fracture of metals at high strain rates was understood as a process through nucleation, growth and coalescence of microscopic voids [1]. It is usually considered that, voids under tension dilate at a higher rate after plastic yielding, then adjoining voids will interact with each other before merging into larger ones. Such procedure is thought to be the mechanism of formation of microcrack out of void-free lattice, which is the most common cause for solid failure. Thus, void interaction has been investigated widely for decades, yet no theories about the details of void dilation and coalescence are universally accepted.

In this paper, molecular dynamics (MD) simulation was used to study a single crystal copper lattice containing two preexisting nanoscale voids subjected to remote uniaxial tension. A criterion was presented to identify the yielding, as well as the coalescence point. Stress distributions around the voids were analyzed in order to find out the critical position where the dislocation was generated first.

2. Methods

In this atomistic-level study of void growth, the simulations were done using embedded atom methods (EAM). The EAM potentials of copper is due to Y. Mishin [2]. The classical equations of motion were integrated using Verlet algorithm with a time step size of 10^{-15}s by LAMMPS [3, 4]. The simulation cell, which contained about 1 million atoms, was a 3-D specimen with edge sizes of 426.7, 426.7 and 57.8Å in Cartesian x, y, and z direction, respectively, at its unstrained state. Periodic boundary conditions were used on all axes, which were along $\langle 100 \rangle$, in order to eliminate the boundary effect, so that there were no free boundaries in the system apart from the voids. About 25500 atoms were removed to create two cylindrical voids with radius

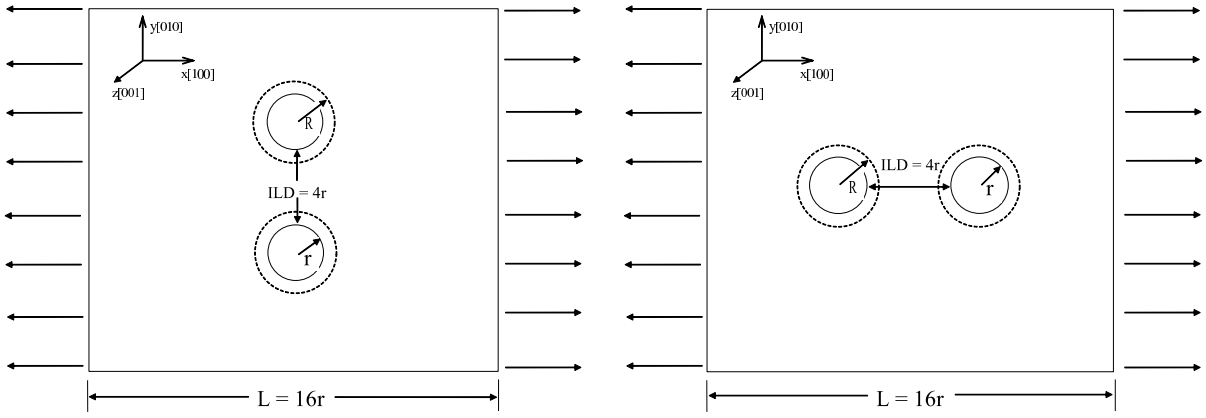

(a) Transverse tension case. (b) Longitudinal tension case.

Figure 1. Geometry of voids contained specimens subjected to uniaxial tension at constant strain rate of 10^9/s. Thickness of each square is 57.8Å. The specified zones we focus are ring circles with r = 28.92Å and R = 32.54Å.

r = 28.92Å. The intervoid ligament distance (ILD) [1], which stands for the shortest surface-to-surface distance between adjoining voids, is 115.68Å. Once the system had been equilibrated using energy minimization by iteratively adjusting atom coordinates, a remote uniaxial tension was exerted on the specimen along x-axis with engineering strain rates of 10^9/s. A constant temperature of 0.01K was obtained by updating positions and velocities each timestep for atoms using a Nose-Hoover temperature thermostat [5]. Two configurations (see Figure 1), characterized by the line connecting centers of two voids was along y or x-axis (called transverse or longitudinal tension case, respectively), were investigated.

3. Results

3.1. Identification of yielding point

Two circle rings around voids were examined, with outside diameter of 65.07Å (see dashed circles in Figure 1), as the specified zones of about 6784 atoms in total. The mean-squared displacements (MSD) of these atoms were computed every 100 steps. MSD is the square of the displacement of each atom, from the original position at the end of equilibration, averaged over all the atoms in the zones of each case. The effect of any drift by the movement of the center of mass of these atoms had been subtracted out before the displacement of each atom was calculated by

$$P_m = \frac{1}{n}\sum_{i=1}^{n}[(P_{ix} - P_{cx} - P_{iox})^2 + (P_{iy} - P_{cy} - P_{ioy})^2], \tag{1}$$

where P_m is MSD of the examined atoms, P_i position of atom i, P_c position of the center of mass of atoms in each zone, P_o position of atom i at the beginning of dilation. In this paper, i and j denote the atoms, while x and y the Cartesian coordinates.

Due to its definition, we thought that the MSD can be used as a token of void volume. According to Potriniche *et al* [6], void volume fraction expanded at a higher speed during plastic stage, thus the rate of MSD was supposed to alter in a similar way. We used

$$\frac{\partial P_m}{\partial \varepsilon_x} = P'_m, \tag{2}$$

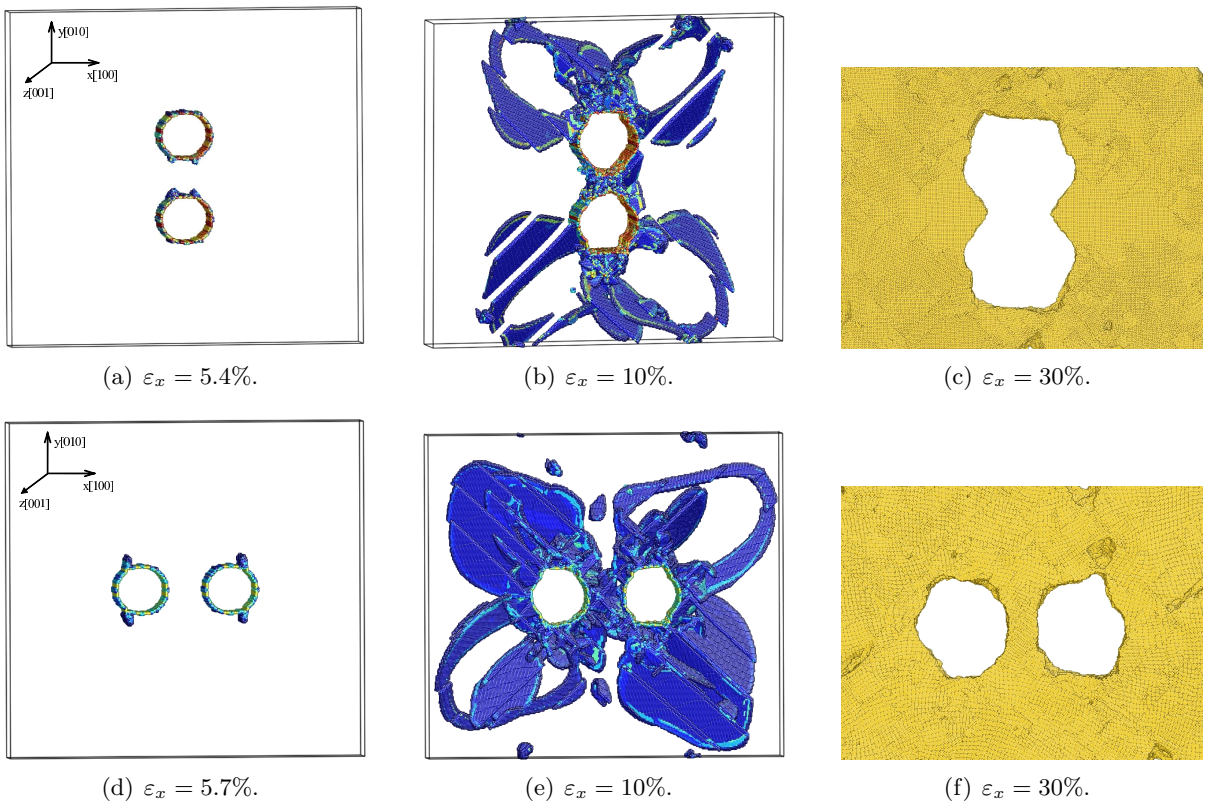

(a) $\varepsilon_x = 5.4\%$. (b) $\varepsilon_x = 10\%$. (c) $\varepsilon_x = 30\%$.

(d) $\varepsilon_x = 5.7\%$. (e) $\varepsilon_x = 10\%$. (f) $\varepsilon_x = 30\%$.

Figure 2. Snapshots of specimens under tension at various stages in both cases. Note that only atoms with CSP ≥ 0.01 are visible in (a), (b), (d) and (e).

where ε_x is engineering strain of the specimen, along the tension direction. P'_m of the specified atoms are plotted in Figure 3. The curves can be observed to deviate away from the elastic behavior at a specific point, when a local maximum of P'_m occurred, corresponding to ε_x of 5.43% in transverse and 5.75% in longitudinal tension case. That was because dislocations were attracted to the surface of voids by image force, resulting in the acceleration of atoms in the inter-surface of voids and deceleration of atoms in the outer-surface of voids [7]. Since the force is in inverse proportion to square of distance, the existence of voids promoted the slip, thus boosted the rate of growth of voids, while energy instability caused by this force generated a high P'_m. Stress distributions around the voids will be investigated in Section 3.3. In order to study this special point further, Atomeye [8] was used to visualize the atomic-level configuration of both specimens. The dislocation was highlighted by centrosymmetry parameter (CSP) [9]. This parameter for each atom is given by

$$c_i = \frac{\sum_{k=1}^{m_i/2} D_k}{2\sum_{j=1}^{m_i} |d_j|^2}, \tag{3}$$

where c_i is the CSP of atom i, m_i the number of its neighbors, D_k and d_j both related to the distance between atom i and its neighbors. c_i is dimensionless with a maximum value of 1. The more distorted the local lattice, the larger c_i. Figure 2(a) and (d), where only atoms with CSP ≥ 0.01 are visible, gave out the snapshot of deformed atoms around the voids at ε_x of 5.4% in transverse and 5.7% in longitudinal tension case. CSP indicated that the dislocation, which was commonly recognized as a sign of plasticity, was just generated.

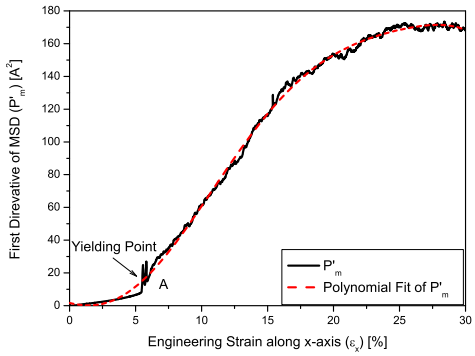

(a) Transverse tension case.

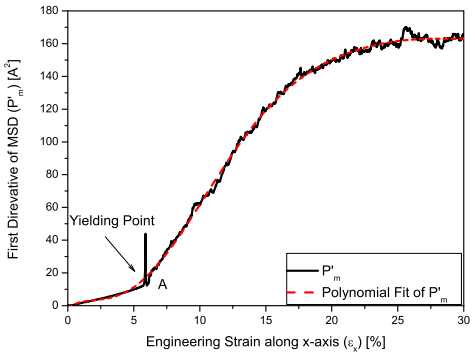

(b) Longitudinal tension case.

Figure 3. Evolution of P'_m (black real curve) and polynomial fit of P'_m (red dashed curve) during tension, with respect to ε_x. Point A is the yielding point.

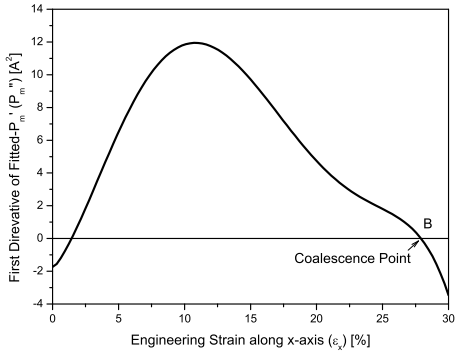

(a) Transverse tension case.

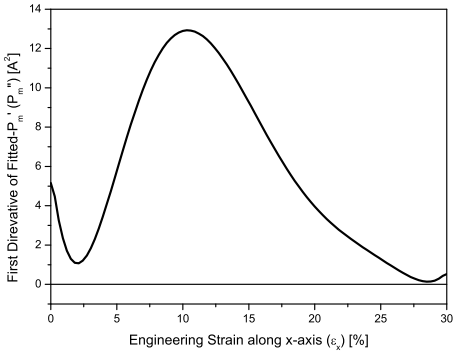

(b) Longitudinal tension case.

Figure 4. Evolution of P''_m during tension, with respect to ε_x. Point B in (a) is the coalescence point.

In both cases, the ε_x here, which marks the inception of plasticity, and the ε_x mentioned above, when a sudden change in the rate of MSD appears, agreed well. Thus P'_m can be regarded as a parameter to distinguish the elastic and plastic zone apart, and point A in Figure 3 can refer to the "yielding point".

3.2. Identification of coalescence point

Identification of coalescence is another confusing question. From Figure 2(c) and (f), when ε_x is of 30% in both cases, one would tell that the void coalescence turned up in transverse tension case while did not in the other. Nevertheless, an index is needed to serve as a quantitative criterion. Void coalescence, i.e., two voids mixing together, creates a larger void. So the interaction mentioned above between dislocations and voids in the vicinity will fade away, making the growth of the void volume slow down. While P'_m can measure the rate of void growth, it tended to be a constant when strain was approaching 30% in Figure 3. In this case, we assumed that such tendency, plus the critical point distinguishing one and two voids apart, might be depicted

by "the rate of rate of void growth" quantitatively. Due to this, polynomial regression was used to fit the data set of P'_m, with respect to ε_x, as the following model:

$$\begin{cases} y = \alpha_0 + \alpha_1 x + \alpha_2 x^2 + \alpha_3 x^3 + \ldots + \alpha_n x^n + \rho \\ \\ \rho \sim N(0, \sigma) \end{cases}, \tag{4}$$

where α_i are coefficients and ρ the error term, which has a normal distribution. α were estimated using a weighted least-square method. The order of the polynomial equation was set to be 6, which can fit the data well but not too sensitive to the precision of α. The $(Fitted - P'_m) \sim \varepsilon_x$ curves were plotted in Figure 3 using red dashed line. Then using

$$\frac{\partial(Fitted - P'_m)}{\partial \varepsilon_x} = P''_m, \tag{5}$$

P''_m were given out, and plotted in Figure 4, versus ε_x. In both cases, P''_m went up as the specimen expanded, then dropped down with $\varepsilon > 11\%$. The difference was this: P'_m in transverse tension case descended to negative with ε_x of 30%, while in the other, still positive under the same ε_x. We considered that it was the coalescence which eliminated the image force effect, that got the rate of P'_m down to negative. On account of this, point B in Figure 4 (a) where $P''_m = 0$ was identified as "coalescence point".

3.3. Shear stress on $(1\bar{1}1)$ plane

Now go back to the specified zones in Figure 1. In consideration of symmetry, only left half part of the circle ring around upper void in transverse, as well as upper half part around left void in longitudinal tension case were studied. In order to analyze the stress distributions, we divided each zone into 18 subregions, using parallel lines along y-axis, with uniform interval of 3.615Å. The stress tensor of the atoms in each zone were calculated by

$$\sigma_{xy} = -\frac{1}{V}\Big(\sum_i \sum_{j>i} r_{ijx} f_{ijy}\Big), \tag{6}$$

where f_{ij} are interatomic forces of atom pairs $\langle ij \rangle$ with corresponding distances r_{ij} [10]. It is commonly believed that dislocations occur preferentially at the plane where the shear stress is maximum [7]. In Figure 2(b) and (e), $[110](1\bar{1}1)$ shear loops emitted from the inter-surface of voids. The shear stress at $(1\bar{1}1)$ along [110] could be calculated by

$$\begin{cases} \tau_N^2 = l^2\Big[\sum_x \Big(\sum_y \sigma_{xy}\Big)^2\Big] - \sigma_N^2 \\ \\ \sigma_N = l^2 \sum \sigma_{xy} \\ \\ l = cos(N, x) = cos(N, y) = cos(N, z) \end{cases}, \tag{7}$$

where N denotes the normal direction of plane $(1\bar{1}1)$ and $l = \sqrt{3}/3$ [11]. Following these equations, the distributions of τ_N in each half circle ring were given out, at ε_x of 5.4% in transverse and 5.7% in longitudinal tension case. τ_N were plotted in Figure 5(c) and (d), with respect to position of center of mass of each subregion, characterized by θ. Note that the max τ_N corresponded to θ of 253° (16th subregion) in transverse, while 100° (11th subregion) in longitudinal tension case. θ in both cases tallied well with where shear loop emitted first in Figure 2(a) and (d), which were marked by shadows in Figure 5(a) and (b). Thus the shear stress theory in [7] can predict position of the first dislocation in our simulation.

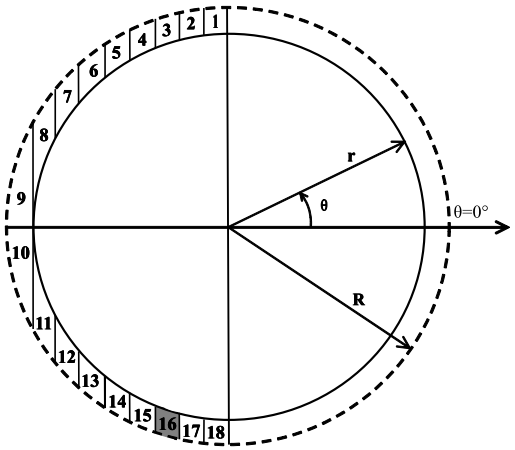

(a) A sketch of 18 subregions around the upper void in transverse tension case.

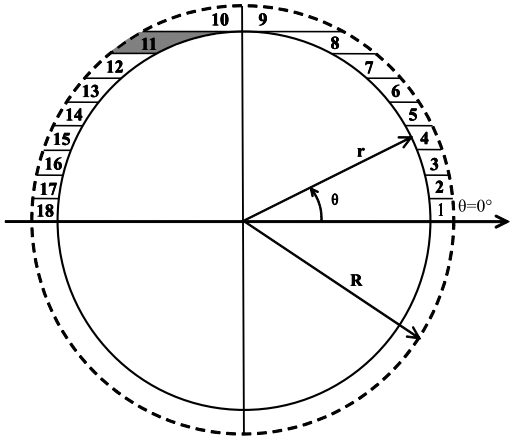

(b) A sketch of 18 subregions around the left void in longitudinal tension case.

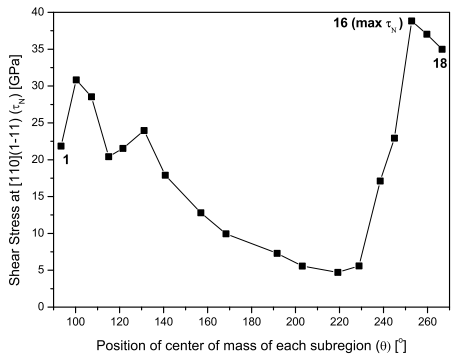

(c) Shear stress of each regions versus their positions in transverse tension case.

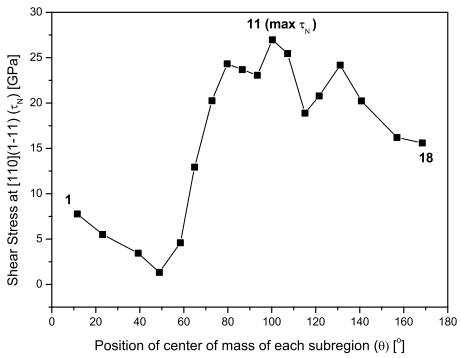

(d) Shear stress of each regions versus their positions in longitudinal tension case.

Figure 5. In each case, the specified zone is a circle ring corresponding to Figure 1, with r = 28.92Å and R = 32.54Å. 18 subregions are labeled by serial number 1–18, whose positions are characterized by θ. Shaded subregions in (a) and (b) marks out where the slip occurred in Figure 2 (a) and (d), respectively.

4. Conclusion

Strain-driven interaction and coalescence of adjoining voids were analyzed, based on molecular dynamics simulation. Two critical parameters which were related to MSD of atoms, were presented during void–void interaction. A sudden change in $P'_m \sim \varepsilon_x$ curve, and the critical point where $P''_m = 0$, were identified as the yielding and coalescence point, respectively. While yielding point was given out, investigations into stress distributions can target the first slip, where the shear stress at slip plane is maximum. These methods can also be used in specimens containing spherical voids, where P_z should be included in Equation 1; and around each void, the specified zone should be a hollow sphere with appropriate R, rather than a circle ring.

References

[1] Seppälä E T, Belak J and Rudd R E 2005 *Phys. Rev.* B **71** 064112
[2] Mishin Y, Mehl M J, Papaconstantopoulos D A, Voter A F and Kress J D 2001 *Phys. Rev.* B **63** 224106
[3] Plimpton S J 1995 *J. Comp. Phys.* **117** 1-19

[4] http://lammps.sandia.gov
[5] Hoover W G 1985 *Phys. Rev. A* **31** 1695-7
[6] Potirniche G P, Horstemeyer M F, Wagner G J and Gullett P M 2006 *International Journal of Plasticity* **22** 257-78
[7] Lubarba V A, Schneider M S, Kalantar D H, Remington B A and Meyers M A 2004 *Acta Mat.* **52** 1397-408
[8] Li J 2003 *Modelling Simul. Mater. Sci. Eng.* **11** 173
[9] Li J 2003 http://mt.seas.upenn.edu/Archive/Graphics/A/Doc/CentralSymmetry.pdf (Accessed: October 25th, 2009)
[10] Zhou M 2003 *Proc. R. Soc. Lond.* A **459** 2347-92
[11] Yang G T 2007 *Introduction to Elasticity and Plasticity* (Berlin: Springer)